



UNICA

UNIVERSITÀ
DEGLI STUDI
DI CAGLIARI



Università di Cagliari

UNICA IRIS Institutional Research Information System

This is the Author's [*accepted*] manuscript version of the following contribution:

Farru, G., Cappai, G., Carucci, A., De Gioannis, G., Asunis, F., Milia, S., Muntoni, A., Perra M., Serpe, A. A cascade biorefinery for grape marc: Recovery of materials and energy through thermochemical and biochemical processes. *Science of the Total Environment*, 846, 157464, 2022.

The publisher's version is available at:

<http://dx.doi.org/10.1016/j.scitotenv.2022.157464>

When citing, please refer to the published version.

© <2022>. This manuscript version is made available under the CC-BY-NC-ND 4.0 license

<https://creativecommons.org/licenses/by-nc-nd/4.0/>

1 A cascade biorefinery for grape marc: recovery of materials and energy through
2 thermochemical and biochemical processes

3

4 Gianluigi Farru ¹, Giovanna Cappai ^{1,2}, Alessandra Carucci ^{1,2}, Giorgia De Gioannis ^{1,2}, Fabiano Asunis ¹,
5 Stefano Milia ², Aldo Muntoni ^{1,2} Matteo Perra ³ and Angela Serpe ^{1,2}

6 ¹ DICAAR - Department of Civil and Environmental Engineering and Architecture, University of Cagliari, Via
7 Marengo 2, 09123 Cagliari, Italy

8 ² IGAG-CNR - Institute of Environmental Geology and Geoengineering, National Research Council, Cagliari,
9 Via Marengo 2, 09123 Italy

10 ³ Department of Life and Environmental Sciences, University of Cagliari, Via Ospedale 72, Cagliari, 09124,
11 Italy

12

13 Corresponding Author: Gianluigi Farru. Email: gianluigi.farru@unica.it.

14

15 Abstract:

16 The agro-industrial sector makes a high contribution to greenhouse gas emissions; therefore, proper waste
17 management is crucial to reduce the carbon footprint of the food chain. Hydrothermal carbonization (HTC) is
18 a promising and flexible thermochemical process for converting organic materials into energy and added-value
19 products that can be used in different applications. In this work, grape marc residues before and after an
20 extraction process for recovering polyphenols were hydrothermally treated at 220 °C for 1 h. The resulting
21 hydrochar and process water were investigated to test an innovative cascade approach aimed at a multiple
22 product and energy recovery based on the integration of HTC with anaerobic digestion. The results show that
23 this biorefinery approach applied to grape marc could allow to diversify and integrate its potential valorisation
24 options. The produced hydrochars possess an increased fixed carbon content compared to the feedstock (up
25 to +70%) and, therefore, can be used in soil, immobilizing carbon in a stable form and partially replacing peat
26 in growing media (up to 5% in case of hydrochar from grape marc after extraction), saving the consumption of
27 this natural substrate. In addition, energy can be recovered from both hydrochar by combustion and from
28 process water through anaerobic digestion to produce biogas. Hydrochars show good properties as solid fuel

29 similar to lignite, with an energy content of around 27 MJ kg⁻¹ (+30% compared to the feedstock). The
30 anaerobic digestion of the process water allowed obtaining up to 137 mL of biomethane per gram of fed COD.
31 Finally, while HTC process waters are suitable for biological treatment, attention must be paid to the presence
32 of inhibiting compounds that induce acute toxic effects in aerobic conditions. The proposed approach is
33 consistent with the principles of circular economy and could increase the overall sustainability and resilience
34 of the agro-industrial sector.

35

36 Keywords: Hydrothermal Carbonization, Biofuel, Soil Amendment, Biomethane, Biorefinery.

37

38 1. Introduction

39 The food supply chain is one of the foundations of human society. Its intrinsically positive role, however, is
40 jeopardized by economic, environmental, and social issues, such as: vulnerability to natural calamities; uneven
41 availability of food and fertile land; overuse of land and water resources and related morphological and
42 hydrographic impacts; threats to ecosystems and loss of biodiversity; overuse of pesticides to increase
43 productivity. Over the last few decades, the food supply chain exacerbated the climate emergency. Globally,
44 the food sector account for more than one-third of total global anthropogenic greenhouse gas emissions (3-7
45 of the 11-19 billion tons of emissions per year) as estimated by the Intergovernmental Panel on Climate change
46 (Crippa et al., 2021). Although land use and production, including fertilizers use, are still the main contributor
47 to agricultural emissions, packaging, transport, "cold chain" activities, processing, and related energy
48 consumption and waste production all play an increasingly large role (Crippa et al., 2021). Reducing the food
49 chain carbon footprint is central to addressing climate change, and proper waste management is of particular
50 importance (Karl & Tubiello, 2021). Improper waste management is pushing the food supply chain to the top
51 of the list of greenhouse gas emitters, as reported by the United Nations Agriculture Agency during the COP26
52 climate conference in Glasgow in 2021. However, the organic nature of most of the residues produced along
53 the food supply chain is suitable for innovative valorization processes consistent with the principles of the
54 circular bioeconomy.

55 It is important to develop processes and approaches to flexibly recover both material and energy resources,
56 in accordance with the needs of local and regional market (Muntoni, 2019). In the case of agro-industrial waste,
57 it is ideal if the recovery of resources addresses concomitant problems, such as the need for renewable energy
58 sources to alleviate increasing energy demands of the food chain, and renewal soil amendments to preserve

59 and restore the carbon balance of the soil (Fryda et al., 2018).

60 Worldwide, 260 million hectolitres of wine were produced in 2020, which is in line with the yearly average
61 production over the last decade. For every 100 kg of grapes, about 70 litres of wine and 18 kg of grape marc
62 are produced. Accordingly, over 6 million tons of grape marc are produced globally every year (OIV -
63 International Organisation of Vine and Wine Intergovernmental Organisation, 2021).

64 The management of such a large amount of biowaste, enriched in water (around 60% by weight) and
65 organic matter (up to 900 g kgTS⁻¹) and characterized by an acidic pH (3-6), and high lignin and polyphenol
66 content is a task that must be faced consistently, made more challenging by the constraints of current
67 environmental and economic policies. Furthermore, management options must consider the seasonality of
68 production since approximately 75% of solid waste is generated during the harvest period (around 2 months).

69 Grape marc is sometimes used as a by-product, e.g., for ruminant animal feeding, although some adverse
70 effects may occur due to the presence of substances such as polyphenols (Baumgärtel et al., 2007; Devesa-
71 Rey et al., 2011; Pinelo et al., 2006). Grape marc can be managed using biological treatments such as
72 anaerobic digestion, with reported methane yields spanning 113 - 420 L CH₄ kgVS⁻¹, or via composting and
73 subsequent use on soil. The relatively high heating value of grape marc (19 - 22 MJ kg⁻¹) would support its use
74 in direct combustion scenarios (Muhlack et al., 2018); however, the high water content makes pre-drying
75 necessary.

76 This study proposes an integrated approach for the sustainable management of grape marc and evaluates
77 valorization options that combine the recovery of materials and energy by coupling different processes such
78 as hydrothermal carbonization and anaerobic digestion, investigating multiple by-products valorization
79 pathways. Hydrothermal carbonization (HTC) is a wet thermochemical process that rapidly converts organic
80 substrates into added-value by-products. Under autogenous pressures and temperatures generally ranging
81 from 180 to 250 °C, a coal-like solid material known as hydrochar and process water are produced, whose
82 characteristics suggest a wide range of potential applications (Libra et al., 2011). During the process, water
83 acts as both the reaction medium and catalyst, making HTC suitable for wet biomass valorization.

84 Hydrothermal carbonization technology is sustainable as it embraces the principles of a circular economy
85 and is a waste management system capable of lowering climate-altering emissions. In its most typical
86 application, biomass-derived hydrochar is used as a fuel for renewable energy production, acting as a neutral
87 combustible and energy-dense carbon source. Being a carbon-enriched solid, hydrochar combustion involves
88 lower CO₂ emissions per unit of energy developed compared to the combustion of the raw material, further
89 offsetting CO₂ emissions. The chemical-physical characteristics of hydrochar make its application interesting

90 also as a soil amendment, able to improve fertility as well as water retention and carbon sink (Funke & Ziegler,
91 2010; Libra et al., 2011; Wang et al., 2018).

92 Besides the hydrochar, the process water may be the bottleneck in view of an industrial up-scaling, since it
93 is still understudied in terms of its sustainable management (Ipiates et al., 2021). Due to the high organic load
94 of process water, it may be a suitable substrate for anaerobic digestion to produce biomethane. Recently,
95 several studies proposed the integration of hydrothermal carbonization with anaerobic digestion as a flexible
96 and circular system to exploit the recovery potential of waste materials (Catenacci et al., 2022; Ipiates et al.,
97 2021).

98 Few studies are reported in literature focusing on grape marc treated via HTC. Basso et al. (2016) treated
99 grape marc (solid-liquid ratio of 1:10) at 180, 220, and 250 °C for 1, 3, and 8 h in a small-scale reactor (50 mL)
100 reporting increasing carbon content and reduced ash and oxygen content in hydrochar (HC). At the same
101 conditions (Baratieri et al., 2015) developed a thermal dynamic model based on the solid yield obtained after
102 HTC of grape seeds. Same results were stated by Nguyen et al. (2022) and Mäkelä et al. (2017) who worked
103 at similar temperatures (180, 220, and 260 °C) for 0.5 h in a 0.5 L pressurized reactor using an initial solid
104 content of 40 and 25 wt%, respectively. Basso et al. (2018) investigated the behavior of grape marc
105 components (seeds and skins) treated at 180, 220, and 250 °C for 0.5, 1, 3, and 8 h using a 50 mL reactor.
106 Mariuzza et al. (2022) applied HTC to different residues, including grape marc, at 220 °C for 1 h in a 50 mL
107 reactor using a solid liquid ratio of 1:5. Other thermochemical processes have also been applied to grape marc:
108 Lin et al. (2021) studied the valorization of this residue and its mixture with other materials (such as cow manure
109 and HCs) via pyrolysis.

110 The available studies, all conducted in small-volume reactors (< 0.5 L), demonstrate the possibility of using
111 the hydrochar from grape marc in different applications; however, no information is yet available on the
112 management of the produced process water and, to the best of our knowledge, on the potential integration of
113 HTC and anaerobic digestion for the valorization of this residue.

114 The specific objective of this work is to assess i) the potential application of the hydrochar produced via
115 HTC from grape marc as a soil improver and solid fuel, and ii) the biological treatability (anaerobic and aerobic)
116 of the process water in view of energetic valorization or disposal. Hydrothermal carbonization was performed
117 on both raw grape marc (GM) and GM after extraction of polyphenols (GM_Ext), compounds that find
118 application in different production sectors.

119 To achieve the study's objective, cascade processes and treatments were applied; HTC tests were carried
120 out at a temperature of 220 °C for 1 h. After HTC, the products were tested through different valorization

121 pathways. The feasibility of hydrochar as a solid fuel and as soil improver or peat substitute was investigated,
122 while assessing the suitability of process water as substrate for energy recovery via AD, or for its treatment in
123 a traditional wastewater plant.

124

125 2. Materials and methods

126 2.1 Feedstock

127 Grape marc (GM) considered in the study consists of skins, stems, and seeds from winemaking with the
128 Cannonau cultivar collected in southern Sardinia (Italy). The GM was dried at 40 °C for about 48 h and stored
129 in the dark at 4 °C in vacuum plastic bags. Considering the significant presence of bioactive molecules in GM,
130 especially polyphenols, their extraction and recovery may be functional to manufacturing nutraceutical and
131 pharmaceutical products for human health (Manca et al., 2020). To this aim, polyphenols separation was
132 carried out through preliminary particle size reduction followed by solid-liquid extraction using a hydroethanolic
133 mixture in a previous study (Perra et al., 2021). Briefly, a part of the dried GM was grinded to obtain a powder
134 with a diameter between 16 and 515 µm, measured with a laser diffraction particle size analyser (Mastersizer
135 3000, Malvern Panalytical Ltd, Worcestershire, UK), using the wet dispersion method and distilled water as
136 dispersant. 100 g of GM was suspended in 1 L of a mixture of ethanol and water (70:30 v/v, density 0.885 g
137 mL⁻¹), and left under stirring conditions in the dark at 25 °C for 48 h. The dispersion was centrifuged two times
138 (30 min, 8000 rpm) to separate solid and liquid fractions. The exhausted GM (GM_Ext) was recovered as
139 feedstock material for the HTC process.

140

141 2.2 Hydrothermal carbonization

142 Hydrothermal carbonization was carried out in a 1.5 L stainless steel pressurized reactor (Berghof, BR-1000).
143 The reactor was equipped with an electric jacket for heating, a thermocouple for the continuous monitoring of
144 the inside temperature, a stirred shaft and a data logging unit connected to a computer where the main
145 operating parameters (inner temperature and autogenic pressure) were continuously recorded. GM and
146 GM_Ext were both treated at 220 °C for 1 h (with a temperature increase of 2 °C min⁻¹). These conditions were
147 selected to balance the conversion performance and the energy consumption. Cellulose and lignin hydrolysis
148 is significant at above 200 °C (Funke & Ziegler, 2010; Libra et al., 2011) and 1 h treatment may assure a proper
149 conversion (high solid yield (Libra et al., 2011) with minimal energy usage. These hypothesis are also confirmed
150 by Lucian & Fiori, (2017) who defined 220 °C for 1 h as the most favourable conditions. The solid material with
151 its moisture content (6.17 ±0.68 wt% and 7.40 ±0.57 wt% for GM and GM_Ext, respectively) was placed in the

152 reactor together with distilled water to achieve a solid content of 10 wt% (1 kg of total input mass) filling the
153 reactor at ca. 75% of its volume. After the input material preparation, the reactor was sealed, and the controller
154 was set to the desired temperature and holding time. Once reactor was kept at 220 °C for 1 h, it was turned off
155 and cooled to room temperature overnight (the temperature profile during the cooling phase is reported in
156 Figure S1 in Supplementary Material). Before unsealing it, the final inner pressure was noted and the gas
157 released evaluated through a column gas meter, based on water displacement method, to estimate the volume
158 produced. To assure a mass balance as precise as possible, all the output materials were carefully weighed
159 before and after each step. The carbonized sludge resulting from the HTC process was separated through a
160 press filter obtaining the solid (hydrochar, HC) and the liquid (process water, PW) phases. The hydrochar was
161 stored in vacuum plastic bags at 4 °C while the process water was vacuum filtered at 0.45 µm and stored in
162 plastic bottles at 4 °C. All tests were carried out three times to ensure replicability. According to the feedstocks,
163 the hydrochars were named HC_GM and HC_GM_Ext and the process water samples PW_GM and
164 PW_GM_Ext.

165 The hydrochars produced were characterized in terms of moisture content, ash content, elemental
166 composition, density, surface chemistry and higher heating value (HHV). The moisture in hydrochar after
167 separation from the liquid phase was estimated by heating three samples (randomly selected from the total
168 mass) to 105 °C. The volatile matter, ash content, and fixed carbon were measured through thermo-
169 gravimetric analysis (TGA – 710, LECO). Further analyses (i.e., CHN/S, HHV, and FT-IR) were conducted
170 on representative dried and milled samples as detailed in the Supplementary Material. Oxygen was evaluated
171 by difference from C, H, N, S, and ash.

172 The liquid phase from the HTC runs was characterized in terms of pH and electrical conductivity (EC), total
173 organic carbon (TOC), and chemical oxygen demand (COD). Details on methods are available in
174 Supplementary Material. All the measurements for both solids and liquids were performed 3 times at least and
175 the results were validated through statistical pairwise t tests (significance level $\alpha = 0.05$) performed using the
176 software JMP (v. 15, SAS).

177

178 2.3 Germination test

179 According to the standard test UNI EN 16086-2:2012-01, Sphagnum peat, previously sieved at 10 mm, was
180 mixed with dried GM, HC_GM, and HC_GM_Ext. 5, 25, and 50 wt% of feedstock or hydrochars were mixed
181 with peat. The samples were named with the codes formed by the initials of the material mixed with the peat
182 and the used amount; to give an example, the sample with the mixture containing peat and 5% hydrochar from

183 grape marc was labelled HC_GM_5%. Moisture was checked and adjusted with the fist test, adding water until
184 squeezing the material with the fist did not produce leaching. Around 50 g of each mixture were placed in 3
185 square Petri dishes and 10 seeds of cress (*Lepidium sativum* L.) were sown at the top of the dish. In addition,
186 3 more Petri dishes filled with only peat were used as a control. One drop of water was added to each seed.
187 Petri dishes were closed with parafilm and stored in an oven at 25 °C for 72 h for incubation with an inclination
188 of 70 – 80° (seeds at the top). After 72 h of incubation, the Petri dishes were opened, the germinated seeds
189 were counted, and the length of the seedlings was measured. The germination rate was defined as the
190 percentage of germinated seeds on the total number of seeds. The results were validated with statistical tests,
191 such as ANOVA and Tukey's HSD test through the statistical software JMP (v. 15, SAS). Several parameters
192 were calculated: average germination rate (AGR), coefficient of variance for germination rate (CVG), average
193 root length per plant (ARLP), coefficient of variance for root length (CVR), average hypocotyl length per plant
194 (AHLPL), coefficient of variance for hypocotyl length (CVH), root length index (RI), and Munoo-Liisa vitality index
195 (MLV).

196

197 2.4 Assessment of material stability

198 Several methods have been proposed to measure biomaterial stability. Among them, respirometric methods
199 based on oxygen consumption are broadly recommended (Sánchez Arias et al., 2012). Electrolytic
200 respirometry is based on the Warburg manometric respirometer and is usually referred to as the Sapromat®
201 system. This system has been extensively applied to estimate O₂ consumption for various purposes/fields:
202 biodegradability of waste and wastewater, toxicity, and inhibition tests, modelling and kinetics of
203 biodegradation, respiration of polluted soils, compost and biologically pretreated waste stability.

204 10 g of pre-humidified HC were placed in a 500 mL glass reaction bottle, connected to an oxygen generator
205 and a pressure control gauge. The bottle rests in a water bath (20 °C). During aerobic degradation,
206 microorganisms consume oxygen and produce an equivalent amount of carbon dioxide. CO₂ is continuously
207 adsorbed by around 5 g NaOH granules, placed in a small container integrated in the reactor bottle, resulting
208 in the establishment of a negative pressure in the bottle. Oxygen is electrolytically produced until the negative
209 pressure is compensated. The amount of produced oxygen is calculated by the required electric energy
210 (according to Faraday's Law), which is recorded in intervals of 36 s by the control unit (Binner et al., 2012)..
211 The tests were run in triplicate.

212 The HC stability was assessed in relation to RA₄ (total oxygen consumption after 4 days), which is the
213 recommended parameter for the estimation of compost stability by the European Union (European

214 Commission, 2001).

215

216 2.5 Assessment of Biochemical Methane Potential (BMP)

217 The BMP measurement is a standard test for determining biogas production from an organic substrate using
218 methanogenic bacteria as the inoculum under optimal batch conditions. This test was applied to the PW
219 produced during HTC for assessing the possibility of conversion into biogas, according to the standard
220 UNI1601755EIT, BMP tests were conducted in brown glass bottles, where methanogenic sludge was mixed
221 with HTC PW. The methanogenic inoculum for biochemical methane potential (BMP) tests was collected from
222 a mesophilic anaerobic digestion plant treating cattle slurry and grass silage located in southern Sardinia (Italy).
223 The amount of sludge and sample was set to allow gas to form in the headspace of the bottles and ensure a
224 food-microorganism ratio (F/M) of 0.5 gCOD gCOD⁻¹ according to the literature (Boulanger et al., 2012; Pagés-
225 Díaz et al., 2020). Methanogenic sludge with D-glucose was used to assess the specific methanogenic activity
226 (SMA, data not shown). A blank was used with only inoculum. No nutrient solution or pH buffer was added to
227 the bottles. The initial pH value was around 7.0 for all samples. All the tests were performed in triplicate. Before
228 the bottles were sealed with airtight caps, they were purged with nitrogen to ensure anaerobic conditions. The
229 sealed bottles were placed in a thermostated shaker (T = 39 ± 1 °C) and kept for 36 days. An average period
230 of 3 days was adopted, slightly shorter at the beginning of the test and longer at the end, to purge the gas
231 produced and accumulated in the reactors. Partial and cumulative biogas production was measured over time.
232 The volume produced was measured through a water-displacement method using a volumetric column, and
233 the gas samples were analyzed using a GC-FID (7890B, Agilent Technologies) equipped with a thermal
234 conductivity detector (TCD) and two stainless columns packed with HayeSep N (80/100 mesh) and Shincarbon
235 ST (50/80 mesh) connected in series.

236 The methane yield at 36 days was calculated as follows (Eq. (1)):

237

$$\text{BMP} = (V_{\text{CH}_4,s} - V_{\text{CH}_4,\text{blank}}) / \text{COD}_s \quad (1)$$

238

239 $V_{\text{CH}_4,s}$ is the volume of methane produced from the PW measured at the end of the test, $V_{\text{CH}_4,\text{blank}}$ is the
240 volume of methane produced from the inoculum measured at the end of the test and COD_s is the mass of
241 soluble COD contained in the volume of added PW.

242 The modified Gompertz equation, based on a sigmoid function, was used to predict the methane production
243 and calculate the kinetic parameters, according to Eq. (2) (Pagés-Díaz et al., 2020). This model was originally
244 developed to describe the slowdown of the batch reactor culture of any microorganism and was modified by
245 Zwietering et al. (1990) by incorporating the classic parameters of maximum concentration, latency time and
246 maximum growth rate. The modified Gompertz model assumes that the methane production is proportional to
247 microbial activity (Nielfa et al., 2015).

$$Y(t)CH_4 = Y_{max}CH_4 \exp \left\{ -\exp \left[\frac{R_{max} \cdot e}{Y_{max}CH_4} (\lambda - t) + 1 \right] \right\} \quad (2)$$

248

249 $Y(t)CH_4$ is the cumulative production yield of CH_4 at time t , $Y_{max}CH_4$ is the maximum theoretical production
250 yield, R_{max} is the maximum production rate, λ is the duration of the lag phase, t is the time and 'e' is the Neperian
251 number. The experimental data were fitted through Eq. (2) using the TableCurve 2D® software (v. 5.01, Systat
252 Software Inc.) through least-squares non-linear regression. The coefficient of determination R^2 was used to
253 preliminary evaluate fitting accuracy of Gompertz model for each experimental dataset.

254

255 2.6 Assessment of acute toxicity

256 A pH-stat titration unit (ANITA, Ammonium NITrification Analyser) was used to assess the acute inhibiting
257 effect of HTC process water on the ammonium-oxidizing bacterial community in activated sludge, as described
258 in Ficara & Rozzi (2001). The tests were carried out in a glass vessel containing 1 L of unacclimated activated
259 sludge (total suspended solids, TSS, 4 g L⁻¹) drawn from the Oristano wastewater treatment plant (Italy). The
260 maximum ammonium-oxidizing capacity of nitrifying biomass was measured in the presence of ammonium as
261 the only substrate, considering the stoichiometric relationship between ammonium oxidation and acidity
262 production, and used as reference. Known volumes of PW_GM and PW_GM_Ext were added to the activated
263 sludge every 20 minutes. The resulting nitrifying activity was compared with the reference and the
264 corresponding inhibition was calculated for each dosage. At the end of the test, nitrification was fully inhibited
265 by allylthiourea to detect the presence of interferences. A dose-response curve was plotted for both PW_GM
266 and PW_GM_Ext according to Eq. (3), and the IC₅₀ (that is the amount of PW that causes 50% acute inhibition
267 of sludge activity) was determined.

$$I(\%) = \left(1 - \frac{1}{1 + \frac{d^a}{b}} \right) 100 \quad (3)$$

268

269 I is the inhibition expressed as percentage, d is the dose in mL L⁻¹ and a and b are curve parameters
270 which are obtained by fitting the experimental data.

271

272 3. Results and discussion

273 3.1 Characterization of feedstock and products

274 The main properties of the two materials used as feedstock for the HTC runs and the characterization of
275 the hydrochars are shown in Table 1. All parameters were evaluated on a dry basis by weight, apart from the
276 moisture content.

277 After the HTC tests, a solid yield (Y) of 62.28 wt db% (± 0.69) was found for GM_Ext, while a slightly lower
278 value of 59.59 wt db% (± 0.52) was obtained in the tests on GM. This is consistent with the extraction process
279 previously applied to GM_Ext, which may have involved the removal of soluble compounds from the solid
280 matrix. Literature reports solid yield ranging from around 50 and 75 wt db% under different operating conditions
281 (Basso et al., 2016; Mäkelä et al., 2017). Mariuzza et al. (2022) obtained a solid yield of 69.2 wt db% (± 1.3) at
282 the same temperature and duration used in our experiments. However, it must be highlighted that the
283 experimental conditions differed for the size reactor (30 times smaller than ours) and for the cooling phase,
284 that was quicker compared to the one applied in our study. The cooling conditions could affect the final yield
285 and properties of the produced materials due to the formation of a secondary char on the surface of the primary
286 char as suggested by different authors (Benavente et al., 2022; Lucian et al., 2018). However, due to the
287 reactor characteristics, we studied the HTC process considering the material deriving from the natural cooling
288 phase without accelerating it. While considering the given limitations related to the cooling phase, our solid
289 yields are placed within the range reported in literature.

290 In comparison to the feedstock, the ash content and the volatile matter in the produced HCs was lower and
291 fixed carbon higher, aspect of interest in view of the use of HC as a fuel and as a carbon replenishment in soil.
292 Regarding the elemental composition, carbon relative content increased, while nitrogen and oxygen ones
293 decreased under the carbonization process. . No significant differences were found between the feedstocks (p
294 > 0.05), apart for volatile matter ($p = 0.023$) and fixed carbon ($p = 0.012$). All parameters analysed in HC

295 reported significant differences compared to the feedstocks ($p < 0.001$), except for hydrogen ($p > 0.05$).
 296 Hydrochars reported significant differences in the solid yield only ($p < 0.001$).

297 Table 1. Main properties of grape marc, extracted grape marc, and hydrochars. STD is reported in brackets.

Material	Code	Solid yield [%]	Moisture [wt%]	Volatile matter [wt%]	Ash [wt%]	Fixed carbon [wt%]	C [wt%]	H [wt%]	N [wt%]	O [wt%]
Grape marc	GM		6.17 (0.07)	71.19 (0.08)	7.64 (0.18)	21.17 (0.10)	49.00 (0.15)	6.09 (0.08)	2.08 (0.13)	35.19 (0.13)
Grape marc (extracted)	GM_Ext		7.40 (0.56)	73.24 (0.17)	8.13 (0.46)	18.64 (0.29)	49.63 (0.29)	5.94 (0.08)	2.09 (0.13)	34.22 (0.23)
Hydrochar from GM	HC_GM	59.59 (0.52)		63.53 (0.48)	3.96 (0.04)	32.51 (0.52)	61.60 (0.60)	6.14 (0.15)	1.85 (0.11)	26.45 (0.76)
Hydrochar from GM_Ext	HC_GM_Ext	62.28 (0.69)		64.95 (1.02)	3.33 (0.01)	31.72 (1.00)	62.46 (0.29)	6.28 (0.12)	1.68 (0.07)	26.25 (0.32)

298 Results are reported on dry basis; moisture on wet basis.

299 To assess potential modifications induced by HTC on the chemical functions of the materials, ATR-FTIR
 300 spectra were recorded on samples before and after the hydrothermal treatment. Figure S2 reports a
 301 comparison between the spectra of the GM powder and of selected seeds, stems, and skin, for starting material
 302 characterization.

303 The spectrum of GM consists of the typical peaks reported for polyphenolic lignocellulosic and flavonoid
 304 compounds found in grape marc (Casazza et al., 2016), together with a contribution of amines as the result of
 305 biogenic decarboxylation processes of amino acids (Grossmann et al., 2007). Details on the peaks attribution
 306 are reported on the spectra (Figure S2). In summary, the typical peaks related to lignin and polyphenols - OH
 307 (ν OH 3300s-br when secondary H-bonding are present, δ OH 1378m, ν PhO 1263s), C-H (aliphatic CH: ν 2980-
 308 2850mw, δ/ρ 1400-1300m; aromatic CH: δ 650-720m), C=C (aliphatic C=C: ν 1650m; aromatic C=C: ν 1540m)
 309 and C-O (ν C=O 1750m; ν C-O 1026s; ν C-O-C 1130m), as well as those typical for amines (ν NH 3313m and
 310 3271m; δ NH 1600m-br; ν CN 1063s), are present (Fan et al., 2012). A comparison of the GM and GM_Ext IR
 311 spectra is reported in Figure 1a, showing no significant modification in the spectrum profile after solvent
 312 extraction. A significant modification of the chemical composition and structure of both feedstock seems
 313 occurring during the HTC process as highlighted by the comparison of the spectra reported in Figure 1b, for
 314 GM and HC_GM, and Figure S3 for GM_Ext and HC_GM. In agreement with the loss of oxygen and nitrogen

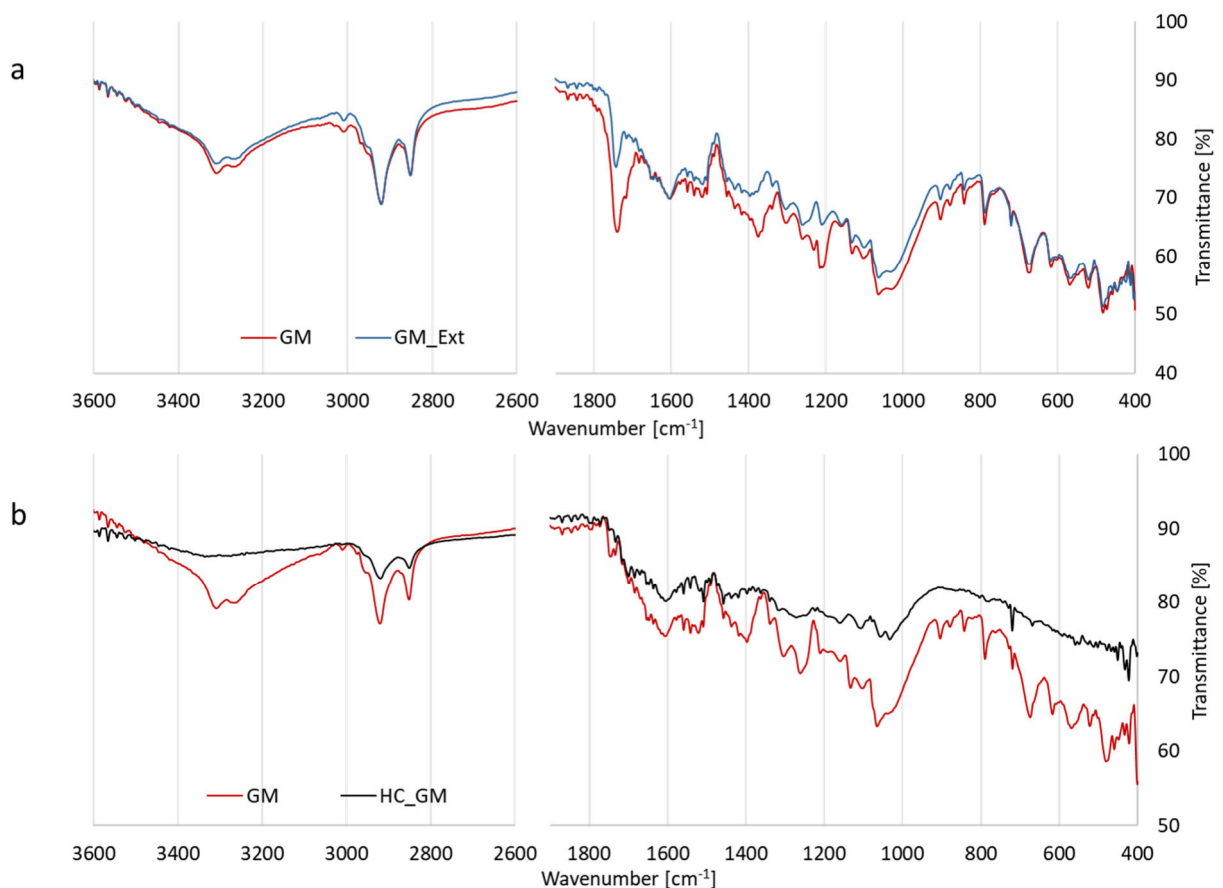
315 found in the samples after HTC, the peaks related to the phenolic moieties of polyphenols and their
316 intermolecular secondary interactions, as well as those of possible carboxylic groups and NH₂ stretching
317 vibrations (ν NH 3271 and 3313 cm⁻¹) are mainly reduced. Correspondingly, peaks typically related to
318 unsaturated aromatic and aliphatic C=C bonds (1650-1598 cm⁻¹) and aromatic CH in bonds (719 cm⁻¹)
319 increased.

320 The main characteristics of the process water are reported in Table 2. The HTC treatment led to an acidic
321 pH and an electrical conductivity (EC) value of around 12 mS cm⁻¹ for both the PW, typical features of the liquid
322 phase from HTC (Funke & Ziegler, 2010; Libra et al., 2011). The total organic carbon (TOC) accounted for
323 9.69 g L⁻¹ for PW_GM and 7.68 g L⁻¹ for PW_GM_Ext. Similarly, the soluble COD was higher in GM than
324 GM_Ext, with values higher than 30 gO₂ L⁻¹. The combined analysis of the characteristics of HC and process
325 water suggests that the preliminary extraction treatment slightly enhances the fixation of carbon in the HC,
326 limiting its release into the PW.

327

328

329



330

331 Fig. 1. FTIR spectra of a) GM and GM_Ext and b) GM and HC_GM.

332 Table 2. Process water characterization (average of triplicates). STD is reported in brackets.

Sample	pH [-]	EC [mS cm ⁻¹]	TSS [g L ⁻¹]	NVSS [g L ⁻¹]	TOC [g L ⁻¹]	COD [gO ₂ L ⁻¹]
PW_GM	4.40 (0.02)	12.52 (0.88)	24.73 (0.01)	9.84 (0.99)	9.69 (0.33)	33.28 (0.42)
PW_GM_Ext	4.37 (0.08)	11.37 (0.16)	21.59 (0.02)	8.90 (0.36)	7.68 (0.48)	31.08 (0.97)

333 EC = electrical conductivity; TSS = total suspended solids; NVSS = non-volatile suspended solids; TOC = total organic
334 carbon; COD = chemical oxygen demand.

335

336 The product mass distribution in the solid, liquid and gas phases observed after the HTC treatment is
337 reported in Table 3. The response to the conditions of the HTC process was similar for the two types of grape
338 marc, regardless of the preliminary extraction. As described in 2.2, the solid content at the beginning of the
339 HTC test was 10%. The treatment resulted in a dramatic reduction of the solid phase with a modest gasification.
340 The solid reduction was likely due to both to dehydration reactions and solid mass solubilisation, the latter
341 resulting in an increased density of the liquid solution. As for the fate of the inorganics, as much as 69.11 and
342 74.49 wt% of the initial ash content of the GM and GM_Ext, respectively, was solubilised in the process
343 water.

344 Table 3 Solid, liquid and gas mass fractions after HTC treatment. STD is reported in brackets.

Phase	GM [wt%]	GM_Ext [wt%]
Solid (Hydrochar)	6.05 (0.07)	6.32 (0.08)
Liquid (Process water)	92.85 (0.13)	92.78 (0.05)
Gas	1.10 (0.06)	0.90 (0.03)

345

346 The results of the characterization analyses of the phases that result from the HTC treatment were used to
347 perform mass balances for the elements carbon and nitrogen according to equation 4.

348

$$M_{IN} = M_{HC\ OUT} + M_{PW\ OUT} + M_{GAS\ OUT} = M_{OUT} \quad (4)$$

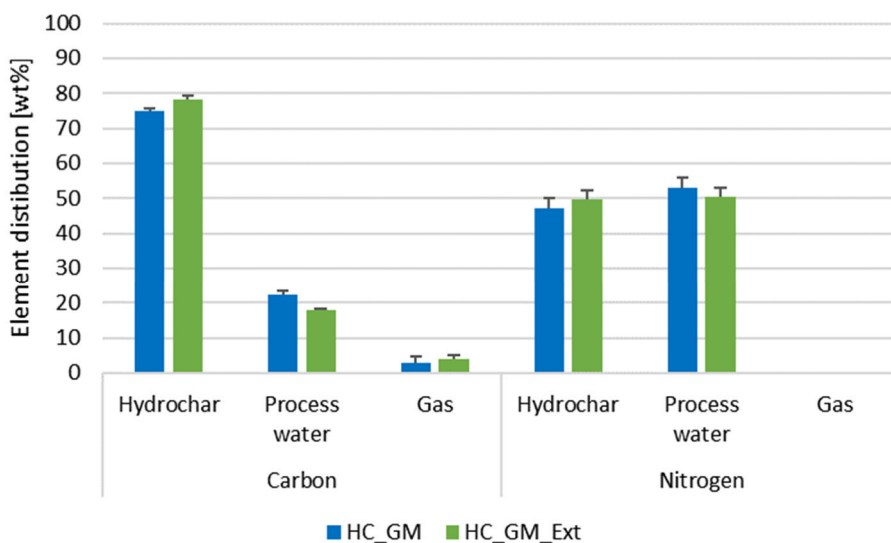
349

350 The carbon and nitrogen distributions in the HTC products are presented in Figure 2, where the gas phase
351 was evaluated considering the measured volume and the density of CO₂ (1.87 kg m⁻³). Most of the carbon is

352 present in the solid phase, to a higher extent in the sample derived from GM_Ext while the carbon dissolved
 353 in the liquid phase is higher for the samples derived from GM. In contrast, nitrogen is almost uniformly
 354 distributed among the solid and liquid phases, as far as the latter is counted as a complement to 100 and
 355 assuming zero nitrogen in the gaseous phase, since the HTC gas is mainly composed by CO₂ (> 95%), CO,
 356 and H₂ (Libra et al., 2011).

357

358



359

360 Fig. 2. Carbon and nitrogen distribution in the HTC products from GM and GM_Ext

361

362

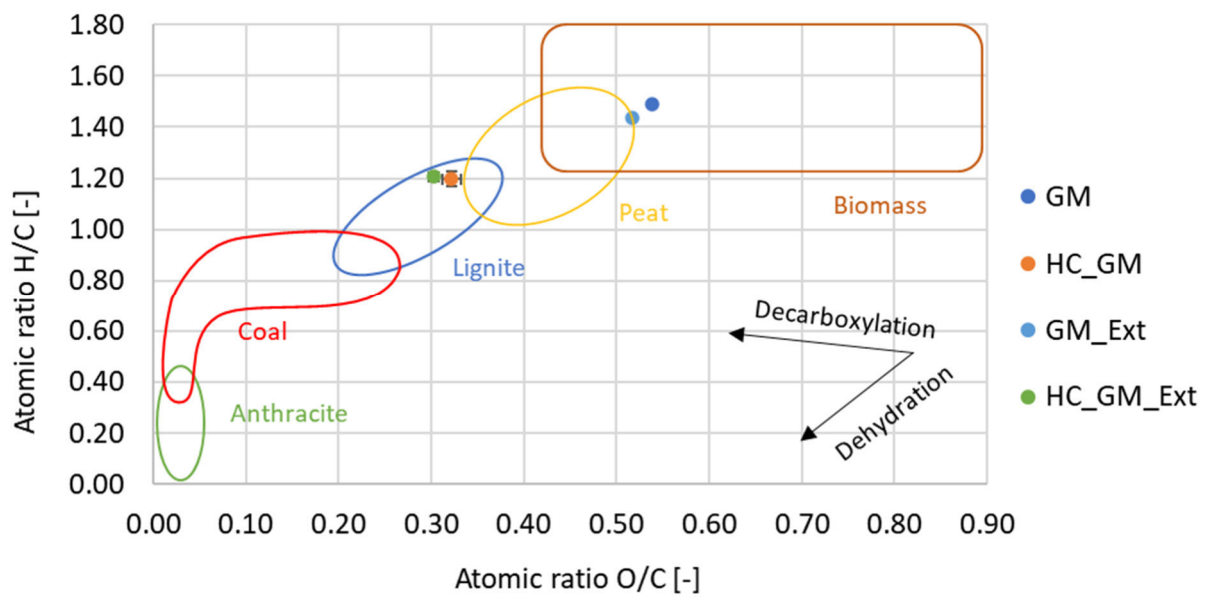
363 3.2 Potential valorization of hydrochars

364 3.2.1 Assessment of the energetic valorization of hydrochars

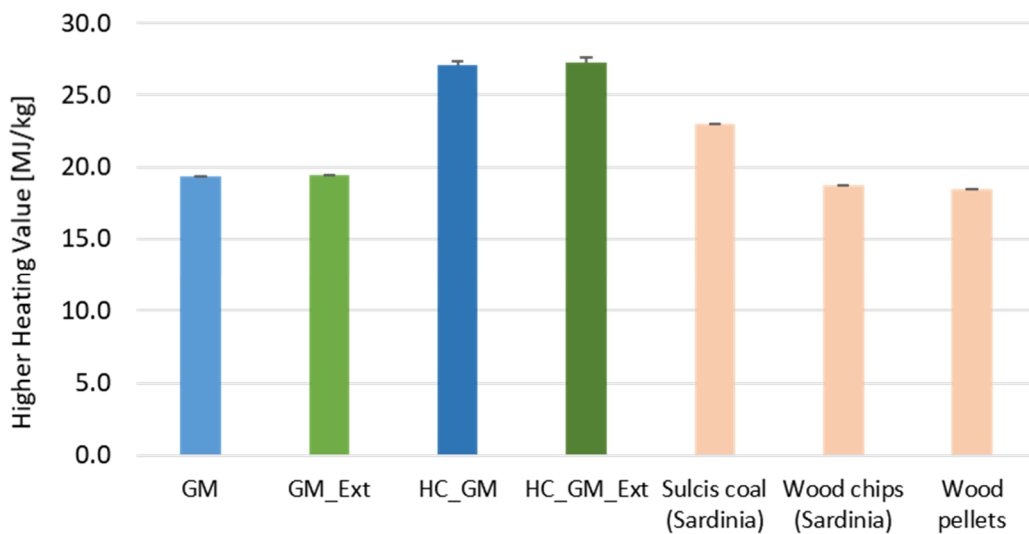
365 In Figure 3, a Van Krevelen diagram, The feedstocks GM and GM_Ext fall within the typical area of
 366 biomass, while the obtained HC, as expected, approach the lignite region as a consequence of the higher
 367 grade of carbonization. Similar results were reported by Mariuzza et al. (2022) with O/C values around
 368 0.3 and H/C approximately 1.1.

369 The Van Krevelen diagram highlights the transformation induced by the process, underlying that the
 370 carbonization decreased both the atomic ratios H/C and O/C as a results of dehydration and
 371 decarboxylation reactions (Funke & Ziegler, 2010; Libra et al., 2011). This is also supported by the FTIR
 372 analyses, which show a reduction in the number of carboxylic and hydroxyl groups due to HTC. The

373 diagram is usually used to define the quality of a solid fuel paired with the assessment of the higher
 374 heating value (HHV) data. The HHV of the samples is shown in Figure 4 along with the HHV of some
 375 common solid fuels. Through HTC, the energy content of the hydrochar (around 27 MJ kg⁻¹) was
 376 increased compared to the feedstock (around 19 MJ kg⁻¹), exceeding the values associated with the solid
 377 fuels considered. Similar HHVs were found by other authors like Mäkelä et al. (2017) and Mariuzza et al.
 378 (2022) who reported values of 26.5 and 26.26 MJ kg⁻¹, respectively.
 379



380
 381 Fig. 3. Van Krevelen diagram of the feedstock (GM and GM_Ext) and hydrochars
 382



384
 385 Fig. 4. HHV of feedstocks, hydrochar and some solid fuels of common use

386

387 3.2.2 Assessment of the potential use of hydrochar as a soil amendment

388 The results of the germination tests are shown in Table 4. When GM and HC_GM results are compared
389 on the basis of the RI and Munoo-Liisa vitality index (which takes into account both the germination and
390 growth aspects normalized by the control), hydrothermal carbonization is able to produce a better
391 substrate for the germination and growth of seedlings. Replacing peat with an equivalent quantity of HC
392 slightly lowers the germination rate, yet leads to longer seedlings compared to the use of raw GM. the
393 best results were achieved for HC_GM_Ext. On the other hand, the higher the concentration of hydrochar,
394 the lower the germination rate, with a high inhibition effect in the samples with 50% peat substitution.
395 However, the presence of hydrochar in a percentage below 25% does not affect the germination
396 significantly, but only the growth of the seedlings. the HC_GM_Ext_5% sample achieved a high RI and
397 MLV values. In contrast, all the other samples have shown inhibition of germination and growth resulting
398 in a lower MLV (less than 80%, which is considered the inhibition threshold as reported in Maunuksela et
399 al. (2012). The lack of inhibition associated with HC_GM_Ext might be due to the preliminary ethanol
400 extraction of GM (Wang et al., 2022). the production of aromatic compounds during the HTC process, as
401 evidenced by the FTIR analysis, does not appear to affect the growth of the seedlings. The statistical
402 analysis derived from one-way ANOVA and Tukey's HSD test is shown in Figure 5 where each letter links
403 samples that are found to be statistically similar ($p < 0.05$). The statistical test confirmed that the samples
404 HC_GM_Ext_5% belong to the same group as the control. It may suggest that the substitution of peat
405 with a 5% hydrochar produced by HTC of extracted grape marc does not affect the seed germination and
406 seedling growth. When hydrochar concentration higher than 5% was added, a detrimental effect on
407 germination was evidenced, indicating that the use in growing medium can be carried out only to a limited
408 extent. However, in a previous study (Farru et al., 2022) we found that some post-treatment can be
409 applied to enhance the germination performance even at higher hydrochar concentrations. Also, it is
410 demonstrated by different authors (Fryda et al., 2018; Lanza et al., 2016, 2018) that the addition of char
411 to soil may replenish and store carbon in soil.

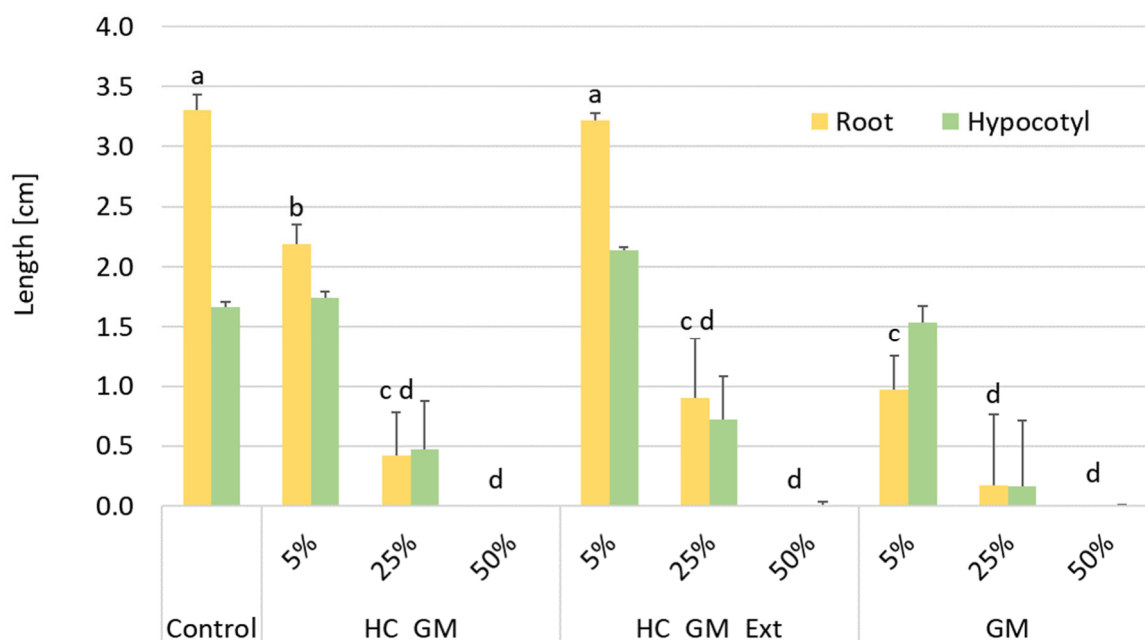
412 Table 4. Main parameters calculated in germination tests for each sample.

Sample	AGR [%]	CVG [%]	ARLP [cm]	CVR [%]	AHLP [cm]	CVH [%]	RI [%]	MLV [%]
--------	---------	---------	-----------	---------	-----------	---------	--------	---------

Control	100	0	3.30	12.58	1.67	4.54	-	-
HC_GM_5%	96.66	5.77	2.19	15.92	1.74	5.47	66.26	63.67
HC_GM_25%	93.33	11.55	0.42	35.46	0.47	40.69	12.82	12.31
HC_GM_50%	0	0	0	0	0	0	0	0
HC_GM_Ext_5%	96.66	5.77	3.22	6.56	2.13	2.58	97.35	94.35
HC_GM_Ext_25%	96.66	5.77	0.89	49.78	0.70	36.30	27.20	26.74
HC_GM_Ext_50%	63.33	15.28	0	0	0.01	2.44	0	0
GM_5%	100	0	0.97	28.22	1.54	13.25	29.47	29.47
GM_25%	46.66	40.41	0.18	59.16	0.17	54.27	5.30	2.12
GM_50%	90	10.00	0	0	0.01	0.00	0	0

413

414



415

416 Fig. 5 Root and hypocotyl length of seedlings in germination tests and statistical results derived by Tukey's HSD
417 test.

418

419 The HC produced from the GM is characterized by a lower respirometric activity, as evidenced by the
420 respirometric index value RA_4 , calculated between the end of the lag phase and the end of the test, of
421 $9.95 \text{ mgO}_2 \text{ gTS}^{-1}$, that is 33% of that associated to HC_GM_Ext ($29.9 \text{ mgO}_2 \text{ gTS}^{-1}$). This feature could be
422 explained by a possible removal of soluble and biodegradable organic compounds during the preliminary
423 phase of extraction. The hypothesis seems to be confirmed by what observed regarding the germination

424 tests; the greater presence of soluble and biodegradable compounds in HC from non-extracted GM and
425 the consequent higher consumption of oxygen could have determined a competition effect between
426 microorganisms and seeds with a prevalence of the former.

427

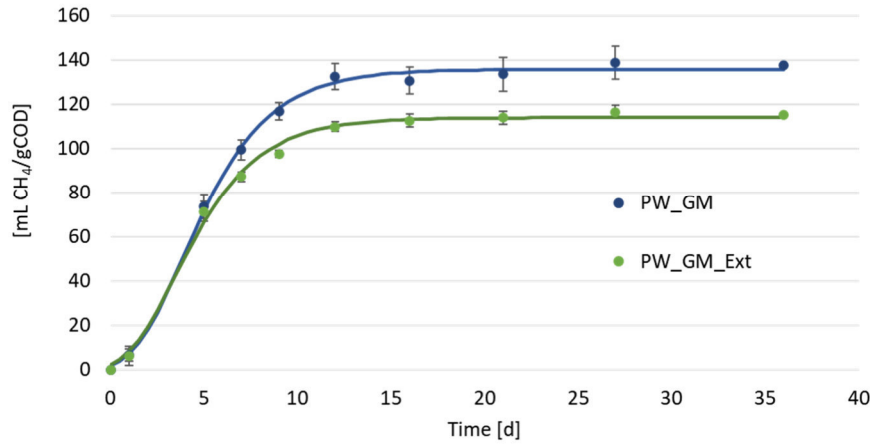
428 3.3 Potential valorization/management of PW

429 3.3.1 Biomethanization Potential of PW

430 The results of the BMP tests performed on the PW samples are summarized in Figure 6 in terms of
431 average cumulative biogas production over time. Methane production started almost immediately in all
432 tests and increased exponentially during the initial phase up to days 12 – 14, albeit at different rates
433 depending on the samples tested. A plateau was reached after about 15 days. The final specific
434 production of methane accounted for 137 and 115 mL CH₄ gCOD⁻¹ for PW_GM and PW_GM_Ext,
435 respectively. These results are comparable to those reported by other authors (Ahmed et al., 2021;
436 Parmar & Ross, 2019) for PW generated from HTC applied to sewage digestate or agricultural waste and
437 fall in the range between 22 and 427 mL CH₄ gCOD⁻¹ indicated by Pagés-Díaz et al. (2020) for HTC liquid
438 phase of organic wastes. The average volumetric methane content in the produced biogas was always
439 higher than 40% v/v. The modified Gompertz model matches the BMP experimental results very closely
440 ($R^2 > 0.99$); the kinetic parameters are reported in Table 5. The process water obtained from HTC of GM
441 and GM_Ext produced methane with a short lag phase of 0.89 – 1.21 days, probably due to the presence
442 of both highly acclimatized microbial consortia and readily degradable organic compounds (Xu et al.,
443 2020). This is confirmed also by the obtained values of R_{max} (16.57 – 19.07 mL CH₄ gCOD_i⁻¹ d⁻¹), similar
444 to those obtained by Gaur et al., (2020) for PW generated from HTC applied to sewage sludge. Pagés-
445 Díaz et al. (2020) reported higher values of λ (0.1 - 7.3 mL CH₄ gCOD_i⁻¹ d⁻¹) and lower values of R_{max}
446 obtained in similar experimental condition for PW generated from HTC applied to lignocellulosic wastes
447 (6 - 13 mL CH₄ gCOD_i⁻¹ d⁻¹), explained by the formation of some toxic compounds released during the
448 HTC. The lower values of maximum CH₄ production rate and Y_{CH_4max} observed for PW_GM_Ext could be
449 linked to the already mentioned possible removal of readily available organic compounds during the
450 preliminary extraction treatment.

451

452



453

454 Fig. 6. Cumulative specific biomethane production from the HTC PW versus time and 95% confidence limits (solid
 455 line indicates Gompertz-model curve).

456

457

Table 5. Kinetic parameters calculated for the BMP tests and associated 95% confidence limits.

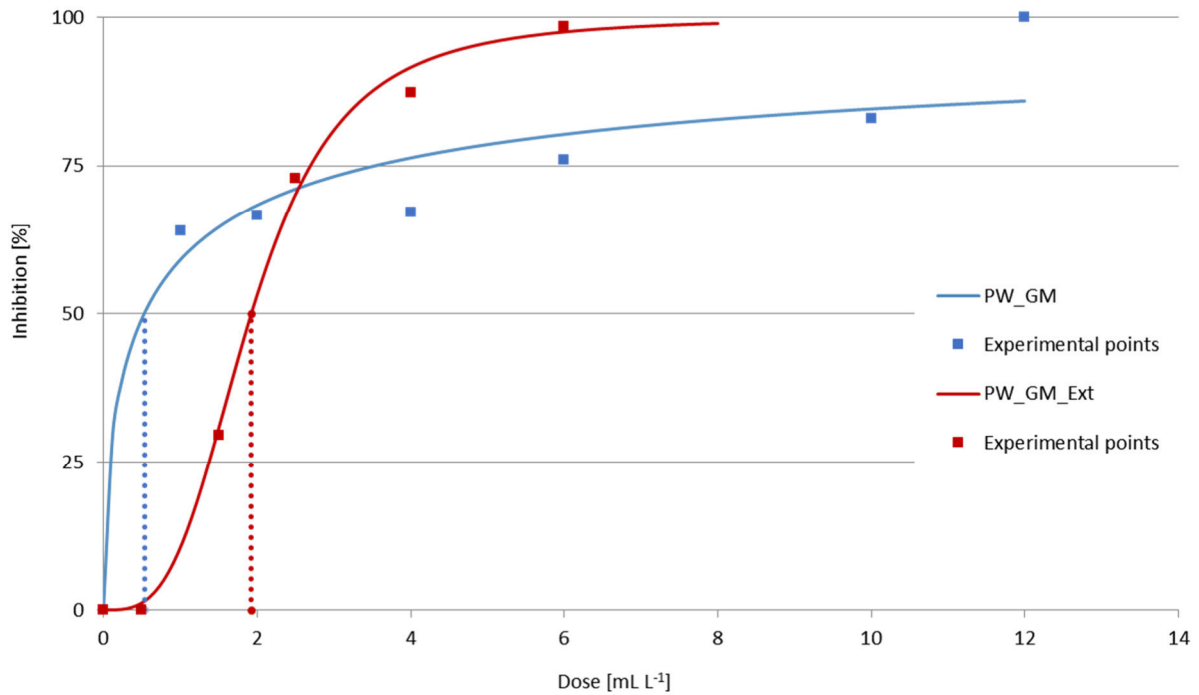
Sample		$Y_{\max}CH_4$ [mL CH ₄ gCOD _i ⁻¹]	R_{\max} [mL CH ₄ gCOD _i ⁻¹ d ⁻¹]	λ [d]	R^2 [-]
PW_GM	Value	135.71	19.07	1.21	0.998
	Lower 95% conf. limit	132.67	16.64	0.64	
	Upper 95% conf. limit	138.75	21.50	1.78	
PW_GM_Ext	Value	113.86	16.58	0.90	0.996
	Lower 95% conf. limit	110.35	13.86	0.19	
	Upper 95% conf. limit	117.38	19.30	1.61	

458

459 3.3.2 Assessment of the potential toxicity of PW in wastewater treatment plants

460 As autotrophic ammonium-oxidizing bacteria are characterized by slow growth rates and high sensitivity
 461 to inhibitors compared to heterotrophs, they can be conveniently employed as test organisms to assess
 462 the potential toxicity of liquid streams to be treated in wastewater treatment plants. Moreover, their
 463 toxicological responses to several chemicals correlate well to that of *Vibrio fischeri* strain NRRL B11177
 464 and methanogens (Ficara & Rozzi, 2001). The assessments performed in the present study showed
 465 potential acute toxicity of PW_GM and PW_GM_Ext at relatively low dosage (the IC₅₀ values were 0.5
 466 and 2.0 mL L⁻¹, respectively) (Figure 7).

467



468

469 Fig. 7. Dose-Response curves showing the acute inhibiting effects of PW_GM and PW_GM_Ext on unacclimated
 470 activated sludge. A sigmoid-function was used to interpolate the experimental data (PW_GM, $a=0.58$, $b=0.694$, $R^2=$
 471 0.944 ; PW_GM_Ext, $a=3.28$, $b=8.547$, $R^2=0.997$).

472

473 Milia et al., (2016b) reported that phenolic compounds might severely inhibit unacclimated activated
 474 sludge even at low concentrations. Accordingly, the higher inhibiting effect of PW_GM is likely due to the
 475 expected higher concentration of phenols. As reported in previous studies, liquid streams containing bio-
 476 recalcitrant compounds with high acute inhibiting effects may be successfully treated using advanced,
 477 low-cost, and efficient biological treatment technologies based on self-aggregated biomass such as
 478 aerobic granular sludge (Milia et al., 2016a), or well acclimated floc-shaped biomass (Milia et al., 2016b).
 479 In this sense, the high potential inhibiting effect observed in our study does not necessarily imply that
 480 aerobic biological treatment of PW_GM and PW_GM_Ext is not feasible, although particular attention
 481 should be paid to biomass selection and acclimation strategies.

482 4. CONCLUSIONS

483 This work demonstrated the possibility of developing a cascading biorefinery scheme for a multi-
 484 purpose valorization of grape marc residues. Hydrothermal carbonization, one of the emerging and most

485 promising technologies for the conversion of biomass and wet materials into added-value by-products,
486 represents the core of this biorefinery approach, in which three consecutive processes were considered
487 for their potential integration: a) the recovery of polyphenols by ethanol extraction, b) the production of
488 added-value materials and energy through thermochemical conversion, and c) the production of CH₄-rich
489 biogas through anaerobic digestion. The potential for the implementation of HTC in an integrated context
490 of waste biorefinery was addressed by applying the process to both raw grape marc and grape marc
491 previously subjected to polyphenol extraction and recovery treatment. The aerobic treatability of process
492 water was also evaluated in view of its final disposal.

493 According to the mentioned strategy, the integrated production of bioproducts, soil amendments, peat
494 substitutes, solid fuels, and biogas was demonstrated.

495 Compared to the feedstock, the produced hydrochars possess an increased content of fixed carbon and
496 a reduced volatile solids and ash content, as well as an increased HHV and improved quality as a solid
497 fuel, suggesting both the feasibility of using HC as a soil amendment for restoring its organic content and
498 exploiting grape marc by producing energy. The outcomes of the germination tests indicated that HC
499 could be used in low concentration to partially replace peat as a substrate for plant growth. This
500 substitution could shorten the supply chain of soil improvers for Mediterranean grape-producing countries
501 that do not have peat deposits.

502 The biogas production from PW assessed during the BMP test indicates that energetic valorization
503 through anaerobic biological process may be a feasible option. Over 90% of the output mass from HTC
504 is PW, therefore, this additional option allows for more extensive exploitation of grape marc and the
505 minimization of the potential environmental impact of PW. In contrast, PW showed toxic effects on aerobic
506 microorganisms suggesting that the feasibility of a traditional aerobic treatment must be carefully
507 evaluated.

508 The results obtained and the comparison with what was observed for the process applied to non-extracted
509 GM, although in need of further investigation, seem to suggest that integration can have positive effects
510 in terms of HC quality as soil improver due to the improved biostability and the reduced phytotoxicity.

511

512 **ACKNOWLEDGEMENTS**

513 The authors gratefully acknowledge Sotacarbo – Sustainable Energy Research Centre and Dr
514 Alessandro Orsini for their valuable support with HHV and TGA analyses.

515

516 Funding source

517 This research did not receive any specific grant from funding agencies in the public, commercial, or
518 not-for-profit sectors.

519 REFERENCES

- 520 Ahmed, M., Andreottola, G., Elagroudy, S., Negm, M. S., & Fiori, L. (2021). Coupling hydrothermal
521 carbonization and anaerobic digestion for sewage digestate management: Influence of
522 hydrothermal treatment time on dewaterability and bio-methane production. *Journal of*
523 *Environmental Management*, 281, 111910. <https://doi.org/10.1016/j.jenvman.2020.111910>
- 524 Baratieri, M., Basso, D., Patuzzi, F., Castello, D., & Fiori, L. (2015). Kinetic and thermal modeling of
525 hydrothermal carbonization applied to grape marc. *Chemical Engineering Transactions*, 43, 505–
526 510. <https://doi.org/10.3303/CET1543085>
- 527 Basso, D., Patuzzi, F., Castello, D., Baratieri, M., Rada, E. C., Weiss-Hortala, E., & Fiori, L. (2016). Agro-
528 industrial waste to solid biofuel through hydrothermal carbonization. *Waste Management*, 47,
529 114–121. <https://doi.org/10.1016/j.wasman.2015.05.013>
- 530 Baumgärtel, T., Kluth, H., Epperlein, K., & Rodehutschord, M. (2007). A note on digestibility and energy
531 value for sheep of different grape pomace. *Small Ruminant Research*, 67(2–3), 302–306.
532 <https://doi.org/10.1016/j.smallrumres.2005.11.002>
- 533 Benavente, V., Lage, S., Gentili, F. G., & Jansson, S. (2022). Influence of lipid extraction and processing
534 conditions on hydrothermal conversion of microalgae feedstocks – Effect on hydrochar
535 composition, secondary char formation and phytotoxicity. *Chemical Engineering Journal*, 428,
536 129559. <https://doi.org/10.1016/j.cej.2021.129559>
- 537 Binner, E., Böhm, K., & Lechner, P. (2012). Large scale study on measurement of respiration activity
538 (AT4) by Sapromat and OxiTop. *Waste Management*, 32(10), 1752–1759.
539 <https://doi.org/10.1016/j.wasman.2012.05.024>
- 540 Boulanger, A., Pinet, E., Bouix, M., Bouchez, T., & Mansour, A. A. (2012). Effect of inoculum to substrate

541 ratio (I/S) on municipal solid waste anaerobic degradation kinetics and potential. *Waste*
542 *Management*, 32(12), 2258–2265. <https://doi.org/10.1016/j.wasman.2012.07.024>

543 Casazza, A. A., Aliakbarian, B., Lagazzo, A., Garbarino, G., Carnasciali, M. M., Perego, P., & Busca, G.
544 (2016). Pyrolysis of grape marc before and after the recovery of polyphenol fraction. *Fuel*
545 *Processing Technology*, 153, 121–128. <https://doi.org/10.1016/j.fuproc.2016.07.014>

546 Catenacci, A., Boniardi, G., Mainardis, M., Gievers, F., Farru, G., Asunis, F., Malpei, F., Goi, D., Cappai,
547 G., & Canziani, R. (2022). Processes, applications and legislative framework for carbonized
548 anaerobic digestate: Opportunities and bottlenecks. A critical review. *Energy Conversion and*
549 *Management*, 263, 115691. <https://doi.org/10.1016/j.enconman.2022.115691>

550 Crippa, M., Solazzo, E., Guizzardi, D., Monforti-Ferrario, F., Tubiello, F. N., & Leip, A. (2021). Food
551 systems are responsible for a third of global anthropogenic GHG emissions. *Nature Food*, 2(3),
552 198–209. <https://doi.org/10.1038/s43016-021-00225-9>

553 Devesa-Rey, R., Vecino, X., Varela-Alende, J. L., Barral, M. T., Cruz, J. M., & Moldes, A. B. (2011).
554 Valorization of winery waste vs. The costs of not recycling. *Waste Management*, 31(11), 2327–
555 2335. <https://doi.org/10.1016/j.wasman.2011.06.001>

556 European Commission. (2001). *Working Document on the Biological Treatment of Biowaste*.
557 http://www.cre.ie/docs/EU_BiowasteDirective_workingdocument_2nddraft.pdf

558 Fan, M., Dai, D., & Huang, B. (2012). Fourier Transform Infrared Spectroscopy for Natural Fibres. In S.
559 Salih (Ed.), *Fourier Transform—Materials Analysis*. InTech. <https://doi.org/10.5772/35482>

560 Farru, G., Dang, C. H., Schultze, M., Kern, J., Cappai, G., & Libra, J. A. (2022). Benefits and Limitations
561 of Using Hydrochars from Organic Residues as Replacement for Peat on Growing Media.
562 *Horticulturae*, 8, 325. <https://doi.org/10.3390/horticulturae8040325>

563 Ficara, E., & Rozzi, A. (2001). PH-Stat Titration to Assess Nitrification Inhibition. *Journal of Environmental*
564 *Engineering*, 127(8), 698–704. [https://doi.org/10.1061/\(ASCE\)0733-9372\(2001\)127:8\(698\)](https://doi.org/10.1061/(ASCE)0733-9372(2001)127:8(698))

565 Fryda, L., Visser, R., & Schmidt, J. (2018). Biochar replaces peat in horticulture: Environmental impact
566 assessment of combined biochar & bioenergy production. *Detritus*, Volume 05-March 2019(0), 1.
567 <https://doi.org/10.31025/2611-4135/2019.13778>

568 Funke, A., & Ziegler, F. (2010). Hydrothermal carbonization of biomass: A summary and discussion of
569 chemical mechanisms for process engineering. *Biofuels, Bioproducts and Biorefining*, 4(2), 160–
570 177. <https://doi.org/10.1002/bbb.198>

571 Gaur, R. Z., Khoury, O., Zohar, M., Poverenov, E., Darzi, R., Laor, Y., & Posmanik, R. (2020).
572 Hydrothermal carbonization of sewage sludge coupled with anaerobic digestion: Integrated
573 approach for sludge management and energy recycling. *Energy Conversion and Management*,
574 224, 113353. <https://doi.org/10.1016/j.enconman.2020.113353>

575 Grossmann, M., Smit, I., & Loehnertz, O. (2007, November 20). *Biogenic amines and grapes: Effect of*
576 *microbes and fining agents*. International symposium of microbiology and food safety, Vilafranca,
577 Spain.

578 Ipiates, R. P., de la Rubia, M. A., Diaz, E., Mohedano, A. F., & Rodriguez, J. J. (2021). Integration of
579 Hydrothermal Carbonization and Anaerobic Digestion for Energy Recovery of Biomass Waste:
580 An Overview. *Energy & Fuels*, 35(21), 17032–17050.
581 <https://doi.org/10.1021/acs.energyfuels.1c01681>

582 Karl, K., & Tubiello, F. N. (2021). *Methods for estimating greenhouse gas emissions from food systems*.
583 FAO. <https://doi.org/10.4060/cb7028en>

584 Lanza, G., Rebensburg, P., Kern, J., Lentzsch, P., & Wirth, S. (2016). Impact of chars and readily
585 available carbon on soil microbial respiration and microbial community composition in a dynamic
586 incubation experiment. *Soil and Tillage Research*, 164, 18–24.
587 <https://doi.org/10.1016/j.still.2016.01.005>

588 Lanza, G., Stang, A., Kern, J., Wirth, S., & Gessler, A. (2018). Degradability of raw and post-processed
589 chars in a two-year field experiment. *Science of The Total Environment*, 628–629, 1600–1608.
590 <https://doi.org/10.1016/j.scitotenv.2018.02.164>

591 Libra, J. A., Ro, K. S., Kammann, C., Funke, A., Berge, N. D., Neubauer, Y., Titirici, M.-M., Fühner, C.,
592 Bens, O., Kern, J., & Emmerich, K.-H. (2011). Hydrothermal carbonization of biomass residuals:
593 A comparative review of the chemistry, processes and applications of wet and dry pyrolysis.
594 *Biofuels*, 2(1), 71–106. <https://doi.org/10.4155/bfs.10.81>

595 Lin, J.-C., Mariuzza, D., Volpe, M., Fiori, L., Ceylan, S., & Goldfarb, J. L. (2021). Integrated
596 thermochemical conversion process for valorizing mixed agricultural and dairy waste to nutrient-
597 enriched biochars and biofuels. *Bioresource Technology*, 328, 124765.
598 <https://doi.org/10.1016/j.biortech.2021.124765>

599 Lucian, M., & Fiori, L. (2017). Hydrothermal Carbonization of Waste Biomass: Process Design, Modeling,
600 Energy Efficiency and Cost Analysis. *Energies*, 10(2), 211. <https://doi.org/10.3390/en10020211>

- 601 Lucian, M., Volpe, M., Gao, L., Piro, G., Goldfarb, J. L., & Fiori, L. (2018). Impact of hydrothermal
602 carbonization conditions on the formation of hydrochars and secondary chars from the organic
603 fraction of municipal solid waste. *Fuel*, 233, 257–268. <https://doi.org/10.1016/j.fuel.2018.06.060>
- 604 Mäkelä, M., Kwong, C. W., Broström, M., & Yoshikawa, K. (2017). Hydrothermal treatment of grape marc
605 for solid fuel applications. *Energy Conversion and Management*, 145, 371–377.
606 <https://doi.org/10.1016/j.enconman.2017.05.015>
- 607 Manca, M. L., Casula, E., Marongiu, F., Bacchetta, G., Sarais, G., Zaru, M., Escribano-Ferrer, E., Peris,
608 J. E., Usach, I., Fais, S., Scano, A., Orrù, G., Maroun, R. G., Fadda, A. M., & Manconi, M. (2020).
609 From waste to health: Sustainable exploitation of grape pomace seed extract to manufacture
610 antioxidant, regenerative and prebiotic nanovesicles within circular economy. *Scientific Reports*,
611 10(1), 14184. <https://doi.org/10.1038/s41598-020-71191-8>
- 612 Mariuzza, D., Lin, J.-C., Volpe, M., Fiori, L., Ceylan, S., & Goldfarb, J. L. (2022). Impact of Co-
613 Hydrothermal carbonization of animal and agricultural waste on hydrochars' soil amendment and
614 solid fuel properties. *Biomass and Bioenergy*, 157, 106329.
615 <https://doi.org/10.1016/j.biombioe.2021.106329>
- 616 Maunuksela, L., Herranen, M., & Tornainen, M. (2012). Quality Assessment of Biogas Plant End Products
617 by Plant Bioassays. *International Journal of Environmental Science and Development*, 305–310.
618 <https://doi.org/10.7763/IJESD.2012.V3.236>
- 619 Milia, S., Mallocci, E., & Carucci, A. (2016a). Aerobic granulation with petrochemical wastewater in a
620 sequencing batch reactor under different operating conditions. *Desalination and Water Treatment*,
621 1–10. <https://doi.org/10.1080/19443994.2016.1191778>
- 622 Milia, S., Porcu, R., Rossetti, S., & Carucci, A. (2016b). Performance and Characteristics of Aerobic
623 Granular Sludge Degrading 2,4,6-Trichlorophenol at Different Volumetric Organic Loading Rates:
624 Water. *CLEAN - Soil, Air, Water*, 44(6), 615–623. <https://doi.org/10.1002/clen.201500127>
- 625 Muhlack, R. A., Potumarthi, R., & Jeffery, D. W. (2018). Sustainable wineries through waste valorisation:
626 A review of grape marc utilisation for value-added products. *Waste Management*, 72, 99–118.
627 <https://doi.org/10.1016/j.wasman.2017.11.011>
- 628 Muntoni, A. (2019). Waste biorefineries: Opportunities and perspectives. *Detritus, Volume 05-March*
629 2019(0), 1. <https://doi.org/10.31025/2611-4135/2019.13791>
- 630 Nguyen, D., Zhao, W., Mäkelä, M., Alwahabi, Z. T., & Kwong, C. W. (2022). Effect of hydrothermal

631 carbonisation temperature on the ignition properties of grape marc hydrochar fuels. *Fuel*, 313,
632 122668. <https://doi.org/10.1016/j.fuel.2021.122668>

633 Nielfa, A., Cano, R., & Fdz-Polanco, M. (2015). Theoretical methane production generated by the co-
634 digestion of organic fraction municipal solid waste and biological sludge. *Biotechnology Reports*,
635 5, 14–21. <https://doi.org/10.1016/j.btre.2014.10.005>

636 OIV - International Organisation of Vine and Wine Intergovernmental Organisation. (2021). *Statistical*
637 *Report on World Vitiviniculture*. [https://www.oiv.int/public/medias/7909/oiv-state-of-the-world-](https://www.oiv.int/public/medias/7909/oiv-state-of-the-world-vitivinicultural-sector-in-2020.pdf)
638 [vitivinicultural-sector-in-2020.pdf](https://www.oiv.int/public/medias/7909/oiv-state-of-the-world-vitivinicultural-sector-in-2020.pdf)

639 Pagés-Díaz, J., Cerda Alvarado, A. O., Montalvo, S., Diaz-Robles, L., & Curio, C. H. (2020). Anaerobic
640 bio-methane potential of the liquors from hydrothermal carbonization of different lignocellulose
641 biomasses. *Renewable Energy*, 157, 182–189. <https://doi.org/10.1016/j.renene.2020.05.025>

642 Parmar, K. R., & Ross, A. B. (2019). Integration of Hydrothermal Carbonisation with Anaerobic Digestion;
643 Opportunities for Valorisation of Digestate. *Energies*, 12(9), 1586.
644 <https://doi.org/10.3390/en12091586>

645 Perra, M., Lozano-Sánchez, J., Leyva-Jiménez, F.-J., Segura-Carretero, A., Pedraz, J. L., Bacchetta, G.,
646 Muntoni, A., De Gioannis, G., Manca, M. L., & Manconi, M. (2021). Extraction of the antioxidant
647 phytocomplex from wine-making by-products and sustainable loading in phospholipid vesicles
648 specifically tailored for skin protection. *Biomedicine & Pharmacotherapy*, 142, 111959.
649 <https://doi.org/10.1016/j.biopha.2021.111959>

650 Pinelo, M., Arnous, A., & Meyer, A. S. (2006). Upgrading of grape skins: Significance of plant cell-wall
651 structural components and extraction techniques for phenol release. *Trends in Food Science &*
652 *Technology*, 17(11), 579–590. <https://doi.org/10.1016/j.tifs.2006.05.003>

653 Sánchez Arias, V., Fernández, F. J., Rodríguez, L., & Villaseñor, J. (2012). Respiration indices and
654 stability measurements of compost through electrolytic respirometry. *Journal of Environmental*
655 *Management*, 95, S134–S138. <https://doi.org/10.1016/j.jenvman.2010.10.053>

656 Wang, G., Yang, Y., Kong, Y., Ma, R., Yuan, J., & Li, G. (2022). Key factors affecting seed germination
657 in phytotoxicity tests during sheep manure composting with carbon additives. *Journal of*
658 *Hazardous Materials*, 421, 126809. <https://doi.org/10.1016/j.jhazmat.2021.126809>

659 Wang, T., Zhai, Y., Zhu, Y., Li, C., & Zeng, G. (2018). A review of the hydrothermal carbonization of
660 biomass waste for hydrochar formation: Process conditions, fundamentals, and physicochemical

661 properties. *Renewable and Sustainable Energy Reviews*, 90, 223–247.
662 <https://doi.org/10.1016/j.rser.2018.03.071>

663 Xu, H., Li, Y., Hua, D., Zhao, Y., Mu, H., Chen, H., & Chen, G. (2020). Enhancing the anaerobic digestion
664 of corn stover by chemical pretreatment with the black liquor from the paper industry. *Bioresource
665 Technology*, 306, 123090. <https://doi.org/10.1016/j.biortech.2020.123090>

666 Zwietering, M. H., Jongenburger, I., Rombouts, F. M., & van 't Riet, K. (1990). Modeling of the Bacterial
667 Growth Curve. *Applied and Environmental Microbiology*, 56(6), 1875–1881.
668 <https://doi.org/10.1128/aem.56.6.1875-1881.1990>

669